Colloid Polym Sci (2013) 291:1863–1870
DOI 10.1007/s00396-013-2917-x

ORIGINAL CONTRIBUTION

Modeling of interface mobility in the description of flow-induced coalescence in immiscible polymer blends

Ivan Fortelný · Josef Jůza

Received: 23 November 2012 / Revised: 16 January 2013 / Accepted: 21 January 2013 / Published online: 16 February 2013

Abstract A new semiempirical equation has been proposed for the rate of approach of highly flattened droplets, applicable in the whole range of the ratios, p, of viscosity of the dispersed droplets and matrix. The equation is utilized to calculate the probability, P_c, that the droplet collision induced by shear or extensional flow is followed by the droplet fusion for systems with Newtonian droplets and Newtonian or viscoelastic matrix. The comparison of the results of these calculations with available experimental data and with the calculation using the trajectory analysis shows that the proposed model of the matrix drainage provides more reasonable results than the broadly applied model of partially mobile interface.

Keywords Flow-induced coalescence · Polymer blends · Matrix drainage · Shear flow · Extensional flow

Introduction

The competition between the droplet breakup and coalescence controls the phase structure evolution during mixing and processing of immiscible polymer blends of the droplets-in-matrix structure. Therefore, the reliable description of the flow-induced coalescence is a necessary condition of the prediction and tailoring of the blend phase structure. Due to its importance for polymer blends and other emulsion-like systems, coalescence is a subject of intensive theoretical and experimental studies [e.g., 1–26]. Coalescence in a flowing polymer blend is a complex event. There is a certain discrepancy between the attempt to describe it precisely and the requirement to achieve, as simply as possible, results which can be efficiently utilized for describing the competition between simultaneous droplet breakup and coalescence. It was recognized that the probability, P_c, that the droplets collision (their touching if all their interactions are neglected) would be followed by their fusion was controlled by the competition between the rate of their approach and the rotation around their common center of inertia [7, 11, 22, 27]. The approach of the droplets is slowed down by the drainage of the matrix trapped between them. During recent years, great attention has been paid to describing and modeling the drainage of the matrix film trapped between colliding drops, including the determination of the condition of the film breakup [6, 7, 12, 13, 16, 17, 28–34]. A recent state of the art of modeling the droplets coalescence in fluids is summarized in [35]. The modern methods of modeling, e.g., boundary integral method, show that the drop shapes develop in a quite complex way (dimple formation) [28, 29, 35]. Calculations are quite difficult and time consuming, especially under conditions reliably modeling the flow. As their results are obtained in numerical form, it is difficult to excerpt dependences on system parameters. Therefore, the dependences of the time of matrix drainage on system parameters are determined by the combination of these results with scaling considerations; they have so far not provided a satisfactory agreement with experiment [28, 29, 31]. Moreover, there are only a limited number of experimental results applicable to the determination of drainage time during the coalescence in shear or extensional flow.

For the reasons discussed above, theories describing the evolution of the shape of coalescing droplets by approximate procedures have so far been used for flowing polymer blends. The importance of coalescence for the evolution of the phase structure in flowing polymer blends was recognized by Elmendorp and Van der Vegt [7, 36]. They

Electronic supplementary material The online version of this article (doi:10.1007/s00396-013-2917-x) contains supplementary material, which is available to authorized users.

I. Fortelný (✉) · J. Jůza
Institute of Macromolecular Chemistry of Academy of Sciences of the Czech Republic, Heyrovského náměstí 2, 16206 Prague 6, Czech Republic
e-mail: fortelny@imc.cas.cz

assumed that the resistance to the droplet approach due to matrix drainage could be expressed as a sum of resistances calculated for hard spherical droplets and for highly flattened droplets with the fully mobile (FMI), partially mobile (PMI), or immobile (IMI) interface. Expressions for FMI, PMI, and IMI were calculated using different boundary conditions [6, 35–37] in the lubrication approximation for the drainage of the matrix between planes with characteristic dimension much larger than their distance. The theory overestimates the matrix resistance due to the consideration of hard spheres instead of viscous droplets, and its duplication for parameters when resistances for spherical and flattened droplets are equal. Janssen and Meijer's theory [11, 37] has frequently been used to describe the flow-induced coalescence in polymer blends as it provides analytical expressions for P_c if the FMI, PMI, or IMI models are considered. The theory is based on the assumption that

$$P_c = \exp\{-t_c/t_i\} \quad (1)$$

where t_c is coalescence time for the approach of droplets from their original distance, h_0, to critical distance, h_c, for the breakup of the thin matrix film, and t_i is interaction time equal to the inversion value of the shear rate, $\dot{\gamma}$. A weak point of this theory is the prediction of a larger P_c (near 1) than that calculated for the spherical droplets of small radius, R, and/or $\dot{\gamma}$. Wang et al. [22] derived a theory of the coalescence of droplets keeping spherical shape through the whole coalescence process until their eventual fusion. Apparently, this theory is applicable if the driving force of coalescence is small and, therefore, possible droplet flattening is negligible. Unfortunately, P_c calculated using the theories of Janssen and Meijer and Wang et al. show quite different dependences on system parameters. Therefore, their using beyond their applicability range can lead to a totally wrong interpretation of experimental results.

Rother and Davis [19] modified the theory of Wang et al. [22] by including the flattening of droplets as a small but singular perturbation. They found that, at a certain particle size and velocity gradient, P_c started to decrease steeply to a negligibly small value. Similar steep decrease in P_c at certain values of these parameters follows also from Janssen and Meijer's theory. Fortelný and Živný [38] used the assumption that the matrix drainage was described by the formula for spherical droplets if the ratio of radii of the flattened part of the droplet and undeformed droplet was smaller than a certain value; a formula for highly flattened droplets was used in the opposite case. Using this assumption, the authors derived a theory for coalescence induced by extensional flow. This theory provided the shape of P_c vs. R dependence similar to that predicted by the Rother and Davis theory. Recently, we have derived the theories of shear-flow- [39] and extensional-flow-induced [40] coalescence. The theories always use the larger of the expressions describing the matrix resistance to the droplets approach for spherical and highly flattened droplets. The dependences of P_c on droplet radius and the rate of the flow of velocity for Newtonian systems have the same shape as those calculated in the previous papers [19, 38].

In the application of Janssen and Meijer's theory [11, 37] and theories based on the switch between expressions for spherical and highly flattened droplets [38–40], the choice of the expression for the resistance of the matrix trapped between flattened droplets to their drainage is an important task. The expressions for the FMI, PMI, and IMI models of the interface were derived for boundary conditions related to the low, moderate, and high ratios of viscosities of the dispersed phase and matrix [6, 37]. Unfortunately, the dependences of individual expressions on system parameters, i.e., the droplet radius, shear or extensional rate, the viscosity of the matrix and droplets, interfacial tension, and critical distance h_c, differ qualitatively and do not pass from one to another with the change of the viscosity ratio. Jeelani and Hartland [12] derived an equation for matrix drainage that passed to the equation for the IMI model at a high viscosity ratio; they predicted decreasing matrix resistance with decreasing viscosity ratio. On the other hand, the dependences of the Jeelani and Hartland (JH) expression on system parameters differ substantially from those of the FMI model. The comparison of P_c calculated using the PMI and JH models shows a strong difference for the viscosity ratios of about 1 [39, 40]. Recently, Gabriele et al. [9] have compared the experimentally determined dependence of droplet radius, R_{ss} (at which P_c for given system parameters falls practically to 0), on the shear rate with predictions following from Janssen and Meijer's theory for the FMI, PMI, and IMI models. They have found that the experimentally determined slopes of the dependence of R_{ss} on the shear rate changes with increasing viscosity ratio continuously from a value predicted for the FMI model to a value for the IMI model.

In the light of the results of Gabriele et al. [9] and considering that the dependence of the matrix resistance to the approach of the droplets on system parameters should change continuously with increasing ratio, p, of the viscosities of the droplets and matrix, we are proposing an expression for the matrix drainage, i.e., the arbitrarily mobile interface (AMI) model, which passes to that of the FMI model at $p \to 0$ and to that for the IMI model at $p \to \infty$.

Construction of the equation describing matrix drainage between highly flattened droplets

We assume that the approach of two highly flattened droplets with $p \to 0$ is described by the equation for the fully mobile interface [6, 7, 11, 27]

$$-\frac{\mathrm{d}h}{\mathrm{d}t}=\frac{2\sigma h}{3\eta_{\mathrm{m}}R} \tag{2}$$

where σ is interfacial tension, h is distance between the surfaces of the droplets, t is time, η_{m} is the viscosity of the matrix, and R is droplet radius. For systems with $p\to\infty$, the droplet approach is described by the equation for the immobile interface [6, 7, 11, 27]

$$-\frac{\mathrm{d}h}{\mathrm{d}t}=\frac{8\pi\sigma^2h^3}{3\eta_{\mathrm{m}}R^2F} \tag{3}$$

where F is the driving force of coalescence. Jeelani and Hartland [12] derived the droplet approach

$$-\frac{\mathrm{d}h}{\mathrm{d}t}=\frac{8\pi\sigma^2h^3}{3\eta_{\mathrm{m}}R^2F}\left(1+\frac{3C}{p}\right) \tag{4}$$

where C is the relative circulation length of the order of unity.

In our construction, we assume that the droplet approach can be described by Eq. 4, where C is an arbitrary function of the system parameters. Equation 4 passes to Eq. 2 for FMI if the following equation is valid for $p\to0$

$$\lim_{p\to0}C=\frac{p}{3}\left(\frac{RF}{4\pi h^2\sigma}-1\right) \tag{5}$$

For $p\to\infty$, Eq. 4 passes to Eq. 3 for the immobile interface for any C independent of p. The following equation meets both the above conditions:

$$C=a\left[1-\exp\left\{-\frac{p}{3a}\left(\frac{RF}{4\pi h^2\sigma}-1+bp\right)\right\}\right] \tag{6}$$

where a and b are dimensionless adjustable parameters. Substitution from Eq. 6 into Eq. 4 leads to the following equation for droplet approach

$$-\frac{\mathrm{d}h}{\mathrm{d}t}=\frac{8\pi\sigma^2h^3}{3\eta_{\mathrm{m}}R^2F}\left\{1+\frac{3a}{p}\left[1-\exp\left\{-\frac{p}{3a}\left(\frac{RF}{4\pi h^2\sigma}-1+bp\right)\right\}\right]\right\} \tag{7}$$

Janssen and Meijer's theory [11] is frequently used to evaluate experimental data. We use their assumption that

$$F=6\pi\eta_{\mathrm{m}}\dot{\gamma}R^2 \tag{8}$$

where $\dot{\gamma}$ is shear rate. After substitution for F into Eq. 7 and its integration, the following equation for coalescence time t_{c} (see Eq. 1) is obtained

$$t_{\mathrm{c}}=\frac{9Ca^2R^2}{4\dot{\gamma}\left(1+\frac{3a}{p}\right)}\left[\frac{1}{2}\left(\frac{1}{h_{\mathrm{c}}^2}-\frac{1}{h_0^2}\right)+\frac{a}{pCaR^2}\ln\left(\frac{1+\frac{3a}{p}-\frac{3a}{p}\exp\left\{-\frac{p}{3a}\left(\frac{3CaR^2}{2ah_{\mathrm{c}}^2}-1+bp\right)\right\}}{1+\frac{3a}{p}-\frac{3a}{p}\exp\left\{-\frac{p}{3a}\left(\frac{3CaR^2}{2ah_0^2}-1+bp\right)\right\}}\right)\right] \tag{9}$$

where capillary number, Ca, is defined as $Ca=\eta_{\mathrm{m}}\dot{\gamma}R/\sigma$.

Coalescence probability in shear and extensional flows

Recently, we have derived the theory of coalescence of Newtonian droplets dispersed in viscoelastic matrix induced by shear [39] or extensional [40] flow. The theory is based on the assumption that the drainage of the matrix between approaching droplets can be described by switching between the expressions for spherical and highly flattened droplets. The expression leading to slower droplet approach is always used. For the considered viscoelastic matrix, F in expressions for the Newtonian system has been substituted with $F+\tau_{\mathrm{m}}\mathrm{d}F/\mathrm{d}t$, where τ_{m} is the relaxation time of the matrix. Final equations describing the approach of spherical and flattened droplets are presented here only. The derivation of these equations is briefly described in the Electronic supplementary material.

For shear flow with unperturbed velocity $\mathbf{u}_0=(\dot{\gamma}y, 0, 0)$, the following equations describing the dependence of the droplet distance, h, on the azimuth, ϕ, have been obtained [39] for spherical

$$-\left(\frac{\mathrm{d}h}{\mathrm{d}\phi}\right)_{\mathrm{sp}}=\frac{2K}{3}\frac{h}{\mathrm{g}(m)}\frac{\mathrm{Q}(\theta,\phi)+\tau_{\mathrm{m}}\dot{\gamma}\mathrm{S}(\theta,\phi)}{\mathrm{D}(\phi)} \tag{10}$$

and for flattened droplets

$$-\left(\frac{\mathrm{d}h}{\mathrm{d}\phi}\right)_{F}=\frac{8h^3}{3KCa^2R^2}\frac{1+\frac{3a}{p}\left[1-\exp\left\{-\frac{p}{3a}\left(\frac{KCaR^2[\mathrm{Q}(\theta,\phi)+\tau_{\mathrm{m}}\dot{\gamma}\mathrm{S}(\theta,\phi)]}{4h^2}-1+bp\right)\right\}\right]}{\mathrm{D}(\phi)[\mathrm{Q}(\theta,\phi)+\tau_{\mathrm{m}}\dot{\gamma}\mathrm{S}(\theta,\phi)]} \tag{11}$$

where K is a function of h and p; g(m) is a function of p and h/R; and D, Q, and S are the functions of azimuth, ϕ, and polar angle, θ. The definitions of these functions can be found in Ref. [39] and in the Electronic supplementary material.

For each initial polar angle, θ_0, the solution of the equation for $dh/d\phi$ constructed by switch between Eqs. 10 and 11, is used to determine the maximum initial angle, ϕ_M, at which colliding droplets fuse. P_c can be determined as

$$P_c = 3\int_0^{\pi/2}\int_0^{\Phi_M} \sin\Phi_0 \cos\Phi_0 \sin^3\theta_0 d\Phi_0 d\theta_0 \quad (12)$$

For the extensional flow with unperturbed velocity $\mathbf{u}_0 = \dot{\varepsilon}(-x, -y, 2z)$, where $\dot{\varepsilon}$ is the deformation rate, the following equations describing the dependence of h on the rotation angle, θ, have been obtained for spherical [40]

$$\left(\frac{dh}{d\theta}\right)_{Sp} = \frac{2K}{3}\frac{h}{g(m)}\frac{Q_e(\theta)+\tau_m\dot{\varepsilon}S_e(\theta)}{D_e(\theta)} \quad (13)$$

and for flattened droplets

$$\left(\frac{dh}{d\theta}\right)_F = \frac{8h^3}{3KCa_e^2R^2}\frac{1+\frac{3a}{p}\left[1-\exp\left\{-\frac{p}{3a}\left(\frac{KCa_eR^2[Q_e(\theta)+\tau_m\dot{\varepsilon}S_e(\theta)]}{4h^2}-1+bp\right)\right\}\right]}{D_e(\theta)[Q_e(\theta)+\tau_m\dot{\varepsilon}S_e(\theta)]} \quad (14)$$

where capillary number, Ca_e, for extensional flow is defined as $Ca_e=\eta_m\dot{\varepsilon}R/\sigma$ and D_e, Q_e, and S_e are the functions of rotation angle, θ, defined in Ref. [40] and in the Electronic supplementary material. The collision of the droplets in extensional flow is followed by their fusion if their distance decreases below h_c until the polar angle θ^* is achieved [40; the Electronic supplementary material]. In calculating $h(\theta^*)$, Eq. 14 for flattened droplets is combined with Eq. 13 for spherical droplets in the same way as for shear flow. Minimum initial polar angle, $\theta_0^{(m)}$, at which $h(\theta^*)=h_c$ should be determined. The probability of coalescence, P_c, for extensional flow can be calculated from the equation [38, 40]

$$P_c = \frac{3\sqrt{3}}{2}\left(\cos\theta_0^{(m)} - \cos^3\theta_0^{(m)}\right) \quad (15)$$

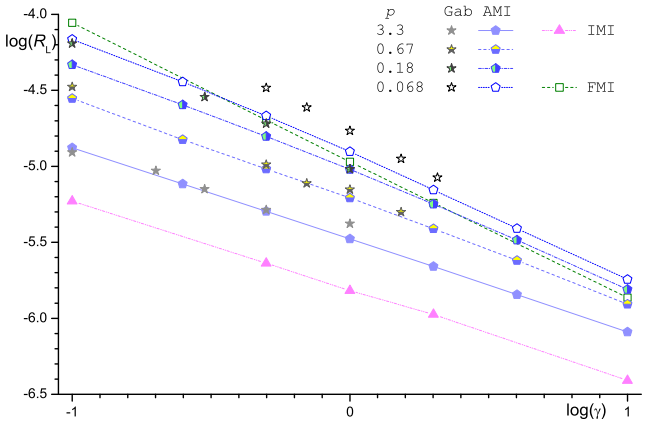

Fig. 1 Comparison of the dependence of drop size R_L on shear rate, calculated using Eq. 11 with a=16 for different viscosity ratios p, with the data of Gabriele et al. [9]; for p=3.3 also with results obtained using IMI model; for p=0.068 also with FMI model. Newtonian matrix, σ=2.8 mN/m, Hamaker constant A=5.10^{-17}J, K_∞=12.24, h_c determined using Eq. 16, h_0=10R. Viscosities: p=3.3, viscosity of the dispersed phase η_d=735 Pa·s, η_m=223 Pa·s; p=0.67, η_d=110 Pa·s, η_m=165 Pa·s; p=0.18, η_d=23.2 Pa·s, η_m=129 Pa·s; p=0.068, η_d=7 Pa·s, η_m=103 Pa·s

ϕ_M and P_c in Eq. 12 for shear-flow-induced coalescence have to be calculated numerically by the procedure

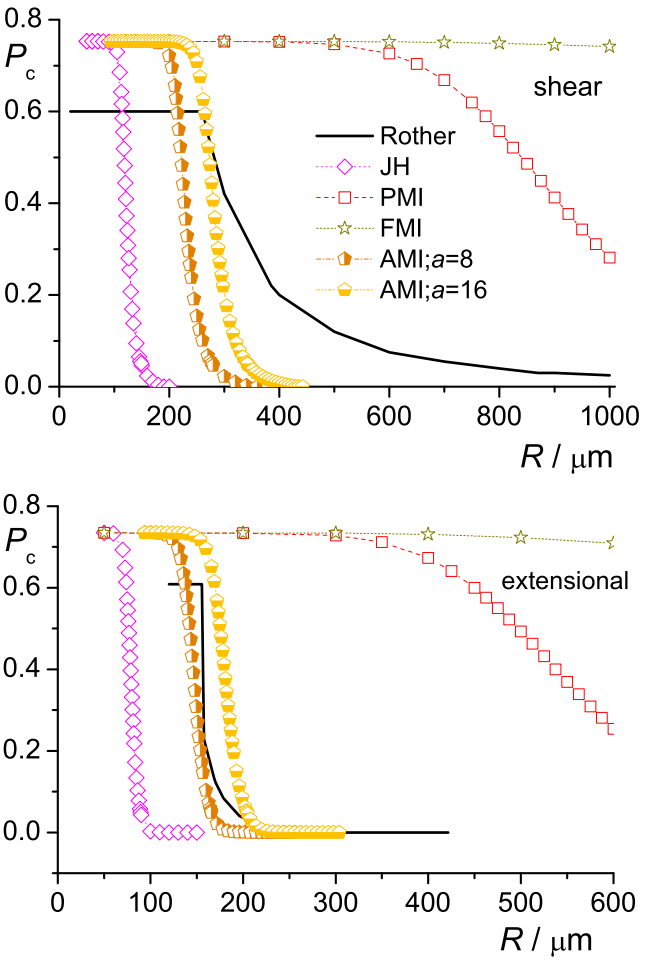

Fig. 2 Comparison of the dependence of coalescence probability P_c on droplets size in shear and extensional flow calculated by Rother and Davis [19] with results of our calculation using FMI, PMI, JH models, and Eq. 11 or 14 with a=8 and a=16. Shear or elongation rate 1 s^{-1}, η_m=0.035 Pa·s, η_d=0.0035 Pa·s, σ=1.9 mN/m, Newtonian matrix, A=5.10^{-21}J, K_∞=12.24, h_c determined by Eq. 16, h_0=10R

described in Refs. [39, 40]. Numerical calculation is also necessary for $\theta_0^{(m)}$ in Eq. 15. The calculation method can be found in Ref. [40]. The critical distance for the droplet fusion, h_c, was calculated using the equation [6, 39]

$$h_c = \left(\frac{AR}{8\pi\sigma}\right)^{1/3} \tag{16}$$

where A is the Hamaker constant. In some cases, h_c=5 nm, a value typical of polymer blends [11, 37], has been used.

The dependence of P_c on system parameters

As the Eq. 7 describing the approach of flattened droplets is semiempirical, the values of constants a and b should be determined from the comparison of calculated P_c with an experiment or with the results of a more fundamental theory. Unfortunately, the amount of experimental data suitable for comparison with our calculation is quite limited. Gabriele et al. [9] determined the dependences of the average droplet radius, at which coalescence started to be undetectable, on shear rate for p from 0.067 to 3.3. In the interpretation of experimental results, Gabriele et al. [9] used the Janssen and Meijer theory [11] and assumed that the limit value of R, R_L, for which the coalescence started to be undetectable, was equal to the characteristic radius, for which t_i=t_c in Eq. 1. Under this condition, P_c=1/e is a non-negligible value. Using this approach, Gabriele et al. [9] found that the slope of the dependence of R_L on $\dot{\gamma}$ complied with the FMI model for p=0.067 and with the IMI model having the h_c independent of R for p=3.3. The slopes for p between these boundary values changed continuously with p. We have tried to use the experimental data of Gabriele et al. [9] for comparison with our calculations. Unfortunately, the dependences of P_c vs. R have a long tail of small but non-zero P_c for the FMI model, and therefore, the results of comparison are sensitive to the choice of the P_c value, for which coalescence is experimentally undetectable.

P_c vs. R dependences calculated for our model can also be compared with the calculations of Rother and Davis by the method of trajectory analysis [19] for the system of ethyl salicylate drops in diethylene glycol (see Figs. 8 and 10 in ref. [19]). This system was characterized by p=0.1.

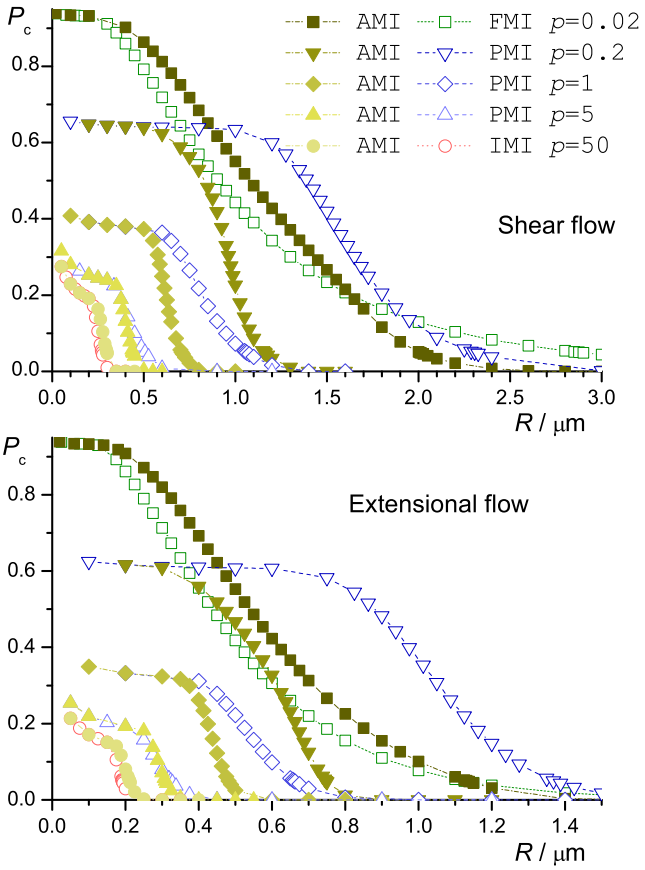

Fig. 3 Comparison of the dependence of coalescence probability P on droplets size in shear flow (*upper plot*) and extensional flow (*lower plot*) calculated using Eq. 11 or 14 and a=8 with those calculated using FMI, PMI, and IMI models for the different ratios p of droplet to matrix viscosity. Newtonian matrix, $\dot{\gamma}(\dot{\varepsilon})$=0.1 s^{-1}, η_m=1 kPa·s, σ=1 mN/m, K_∞=12.24, h_c=5 nm

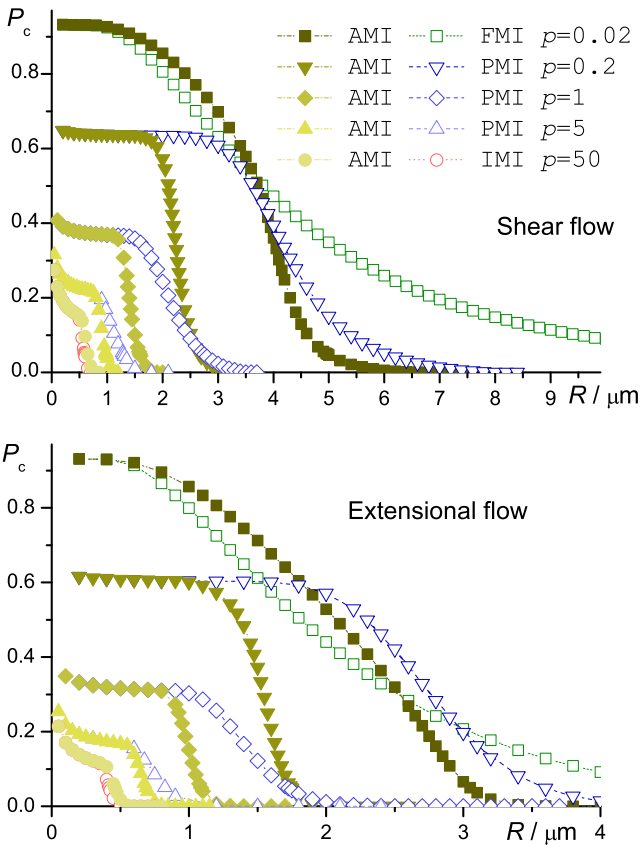

Fig. 4 Same dependences and parameters as in Fig. 3, with the exception of σ=5 mN/m

The comparison of the dependences of P_c on R calculated by our method for the Newtonian systems with the data of Gabriele et al. [9] and Rother and Davis [19] has been used for the determination of the parameters a and b. The results of our calculations (not shown for brevity) are only slightly sensitive to the value of b. It should be mentioned that the term bp has been added to the exponent to avoid the unphysical behavior of the expression in Eq. 7 for $RF<4\pi h^2\sigma$ at $p\rightarrow\infty$. Therefore, the value $b=1$ is used in our calculations.

The value of a affects the shape of the P_c vs. R dependence more substantially than the value of b. For the proposed model, P_c has been found to approach, with increasing p, the values for the IMI model faster for smaller values of a. The approach of P_c to the values for the FMI model, with decreasing p, is faster for larger values of a. Generally, the decrease in P_c with R in the region of larger R is much steeper for our model than for the FMI model, even for large a and small p.

The dependences of R_L on $\dot{\gamma}$ determined experimentally [9] and calculated under the condition $P_c(R_L)=0.05$ are compared in Fig. 1. For $p=0.068$, the experimentally determined slope of the dependence agrees with the slope calculated for the FMI model. The absolute value of the slope calculated according to our model is somewhat smaller. For $p=0.18$, the absolute value of the slope calculated according to our model is also smaller than that determined experimentally. For $p=0.67$, the slopes calculated using our model and experimentally determined are in good agreement. For $p=3.3$, the slopes calculated for our and IMI models agree very well. However, the absolute values of the calculated slopes are somewhat larger than those determined experimentally.

The dependences of P_c on R calculated by Rother and Davis [19] and by our method are compared in Fig. 2. It should be mentioned that for $p<1$, our calculation method leads systematically to a larger P_c than the method of Rother and Davis in the region of small R [40]. Comparison of Fig. 2a with Fig. 9 in Ref. [39] shows that the difference between these methods is smaller if K is calculated using Eq. (S2) in the Electronic supplementary material than for constant K equal to K_∞. Figure 2 clearly shows that the calculations using Eq. 7 with $a=8$ or 16 for the approach of flattened droplets correspond to the results of Rother and Davis much better than those using the PMI model. A decrease in P_c with R in the region of R, where the droplet flattening starts, is somewhat steeper for our model than for that of Rother and Davis. The decreasing part of the P_c vs. R curve (except the region of very small P_c) calculated according to the Rother and Davis theory lies between our

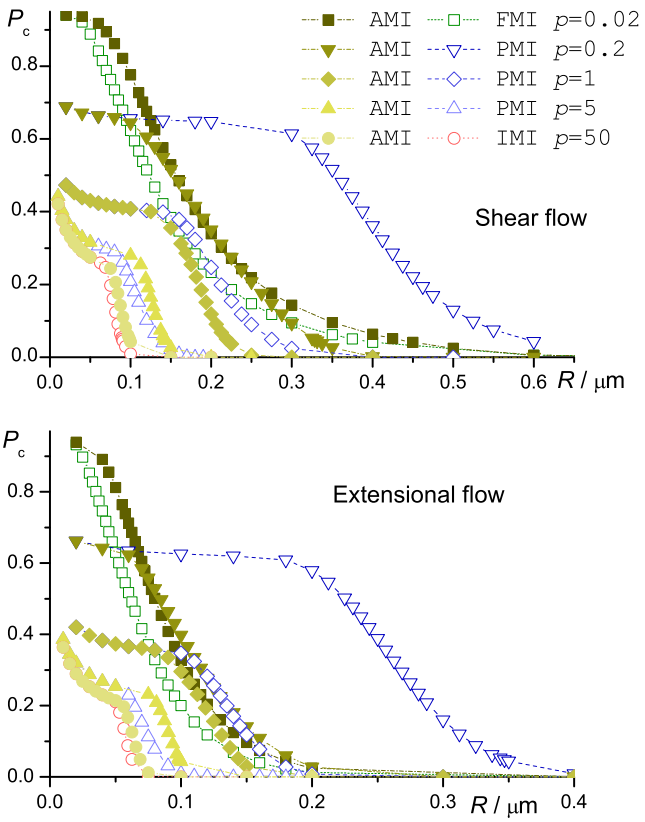

Fig. 5 Same dependences and parameters as in Fig. 3, with exception of $\dot{\gamma}(\dot{\varepsilon})=1\ s^{-1}$

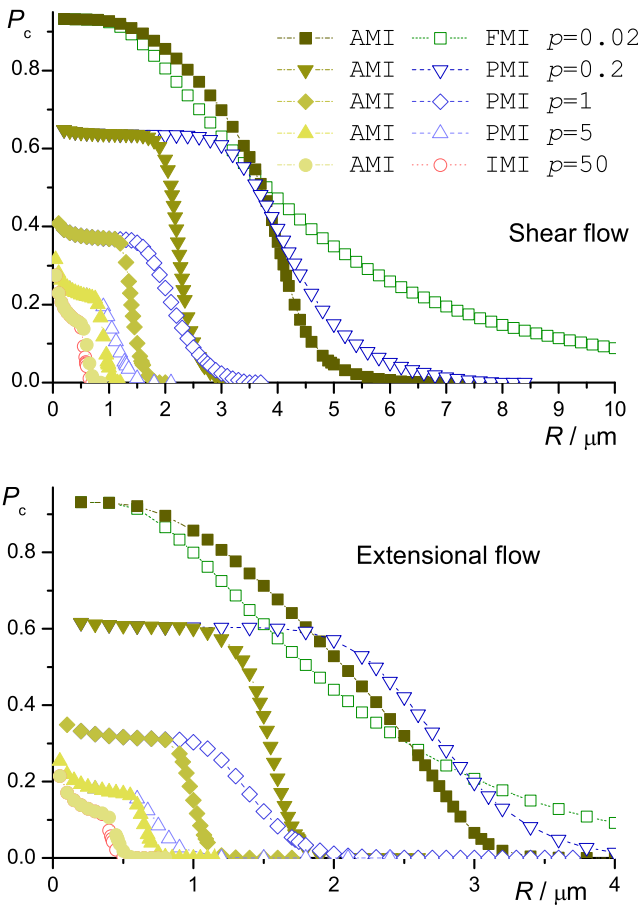

Fig. 6 Same dependences and parameters as in Fig. 3, with the exception of $\dot{\gamma}(\dot{\varepsilon})=0.02\ s^{-1}$

calculations for a=8 and 16 for the extensional flow and corresponds to our calculation with a=16 for the shear flow.

The comparison of the dependences of P_c on R calculated for Newtonian droplets in the Newtonian liquids in the shear flow for our model of the matrix drainage with the FMI, IMI, and PMI models for small, large, and medium p, respectively, is provided in Figs. 3, 4, 5, and 6 for shear or extensional rates of 0.02, 0.1, and 1 s^{-1} and interfacial tensions of 1 and 5 mN/m. The viscosity of the matrix η_m=1,000 Pa·s has been considered. We believe that these parameters are typical of polymer blends in the measurements of their rheological properties. It follows from these figures that the relations between P_c calculated for the various models of the interface mobility are similar for the shear and extensional flows and for all chosen parameters. For a=8, the dependence for our model is close to the dependence for the IMI model at p=50. For p=0.02, our model leads to a somewhat larger P_c for medium R and to smaller P_c for large R than the FMI model. For p=0.2, Fig. 3 demonstrates that the PMI model apparently overestimates P_c because, in a certain range of R, this P_c is larger than P_c calculated for the FMI model at p=0.02. The decrease in P_c with R is somewhat slower for the PMI model than for our model at p=1. For p=5, the dependences of P_c on R for our model and the PMI model are similar. Overestimation of R, at which P_c starts to decrease for low values of p, in the PMI model increases with increasing shear or extensional rate and seems to decrease with σ. The inadequacy of the PMI model for p>>1 was demonstrated and discussed in our preceding paper [39].

Figure 4 shows that the increase in interfacial tension deteriorates the accordance between the AMI and FMI models for lower P_c (higher R). As it can be seen in Fig. 5, under higher shear rates, PMI provides results shifted in comparison with the IMI, FMI, and AMI methods.

It can be concluded that our model of the matrix drainage between flattened droplets provides a reasonable agreement with available experimental data in the whole range of p, and a=8 and b=1 seem to be reasonable values of the adjustable parameters. However, their values can be corrected after more extensive comparison of this model with experimental results. It should be mentioned that the above analysis has shown that the PMI model, broadly used for the description of the flow-induced coalescence in polymer blends, has not provided reasonable results in many cases.

Conclusion

A new semiempirical model of the matrix drainage between flattened droplets applicable in the whole range of viscosity ratio, p, has been proposed. The model provides a better agreement of the coalescence probability P_c, calculated using the procedure developed in our preceding papers [39, 40], with experimental data [9] and with P_c calculated using the trajectory analysis [19] than the PMI model so far broadly used for the description of the flow-induced coalescence in polymer blends.

Acknowledgments The authors are grateful for the financial support of the Grant Agency of the Czech Republic (grant no. P106/11/1069).

References

1. Al-Mulla A, Gupta RK (2000) Droplet coalescence in the shear flow of model emulsions. Rheol Acta 39:20–25
2. Börschig C, Arends P, Gronski W, Friedrich C (2000) Kinetics of flow-induced coalescence and form relaxation in polymer blends as studied by rheo small angle light scattering. Macromol Symp 149:137–143
3. Burkhart BE, Gopalkrishnan PV, Hudson SD, Jamieson AM, Rother AM, Davis RH (2001) Droplet growth by coalescence in binary fluid mixtures. Phys Rev Letters 87(9):098304–1–098304–4
4. Caserta S, Simeone M, Guido S (2006) A parameter investigation of shear-induced coalescence in semidilute PIB-PDMS polymer blends: effects of shear rate, shear stress, volume fraction, and viscosity. Rheol Acta 45:505–512
5. Chen D, Cardinaels R, Moldenaers P (2009) Effect of confinement on droplet coalescence in shear flow. Langmuir 25:12885–12893
6. Chesters AK (1991) The modeling of coalescence processes in fluid-liquid dispersions: a review of current understanding. Trans Inst Chem Eng 69:259–270
7. Elmendorp JJ, Van der Vegt AK (1986) A study on polymer blending microrheology: part IV. The influence of coalescence on blend microrheology origination. Polym Eng Sci 26:1332–1338
8. Filippone G, Netti PA, Acierno D (2007) Microstructural evolution of LDPE/PA 6 blends by rheological and rheo-optical analyses: influence of flow and compatibilizer on break-up and coalescence processes. Polymer 48:564–573
9. Gabriele M, Pasquino R, Grizzuti N (2011) Effects of viscosity-controlled interfacial mobility on the coalescence of immiscible polymer blends. Macromol Mater Eng 296:263–269
10. Hsu AS, Roy A, Leal LG (2008) Drop-size effects on coalescence of two equal-sized drops in a head-on collision. J Rheol 52:1291–1310
11. Janssen JMH, Meijer HEH (1995) Dynamic of liquid-liquid mixing: a 2-zone model. Polym Eng Sci 35:1766–1780
12. Jeelani SAK, Hartland S (1994) Effect of interfacial mobility on thin film drainage. J Colloid Interface Sci 164:296–308
13. Leal LG (2004) Flow induced coalescence of drops in a viscous fluid. Phys Fluids 16:1833–1851
14. Li Y-Y, Chen Z-Q, Huang Y, Sheng J (2007) Morphology development in polypropylene/polystyrene blends during coalescence under shear. J Appl Polym Sci 104:666–671
15. Lyu S-P, Bates FS, Macosko CW (2000) Coalescence in polymer blends during shearing: experimental studies. AICHE J 46:229–238
16. Lyu S-P, Bates FS, Macosko CW (2002) Modeling of coalescence in polymer blends. AICHE J 48:7–14
17. Milner ST, Xi H (1996) How copolymers promote mixing of immiscible homopolymers. J Rheol 40:663–687
18. Okamoto K, Iwatsuki S, Ishikawa M, Takahashi M (2008) Hydrodynamic interaction and coalescence of two droplets under large step shear strains. Polymer 49:2014–2017

19. Rother MA, Davis RH (2001) The effect of slight deformation on droplet coalescence in linear flows. Phys Fluids 13:1178–1190
20. Rusu D, Peuvrel-Disdier E (1999) In situ characterization by small angle light scattering of the shear-induced coalescence mechanisms in immiscible polymer blends. J Rheol 43:1391–1409
21. Søndergaard K, Lyngaae-Jørgensen J (1996) Coalescence in an interface-modified blend as studied by light scattering measurements. Polymer 37:509–517
22. Wang H, Zinchenko AZ, Davis RH (1994) The collision rate of small drops in linear flow fields. J Fluid Mech 265:161–188
23. Wildes G, Keskkula H, Paul DR (1999) Coalescence in PC/SAN blends: effect of reactive compatibilization and matrix phase viscosity. Polymer 40:5609–5621
24. Yu W, Zhou C (2007) Coalescence of droplets in viscoelastic matrix with diffuse interface under simple shear flow. J Polym Sci, Part B: Polym Phys 45:1856–1869
25. Perilla JE, Jana SC (2004) A time-scale approach for analysis of coalescence in processing flows. Polym Eng Sci 44:2254–2265
26. Verdier C (2000) Coalescence of polymer droplets: experiments on collision. Cr Acad Sci IV-Phys 1(1):119–126
27. Fortelný I (2006) Theoretical aspects of phase morphology development. In: Harrats C, Thomas S, Groeninckx G (eds) Micro- and nanostructured multiphase polymer blend systems: phase morphology and interfaces. Taylor and Francis, Boca Raton, pp 43–90
28. Baldessari F, Leal LG (2006) Effect of overall drop deformation on flow-induced coalescence at low capillary numbers. Phys Fluids 18:013602-1–013602-20
29. Yoon Y, Baldessari F, Ceniceros HD, Leal LG (2007) Coalescence of two equal-sized deformable drops in an axisymmetric flow. Phys Fluids 19:102102-1–102102-24
30. Vannozzi C (2012) Relaxation and coalescence of two equal-sized viscous drops in a quiescent matrix. Journal of Fluid Mechanics 694:408–425
31. Kaur S, Leal LG (2009) Three-dimensional stability of a thin film between two approaching drops. Phys Fluids 21:072101-1–072101-17
32. Zdravkov AN, Peters GWM, Meijer HEH (2006) Film drainage and interfacial instabilities in polymeric systems with diffuse interfaces. J Colloid Interface Sci 296:86–94
33. Tufano C, Peters GWM, Meijer HEH, Anderson PD (2010) Effects of partial miscibility on drop-wall and drop-drop interactions. J Rheol 54:159–183
34. Yu W, Zhou C (2007) Coalescence of droplets in viscoelastic matrix with diffuse interface under simple shear flow. J Polym Sci, Part B: Polym Phys 45:1856–1869
35. Janssen PJA, Anderson PD (2011) Modeling film drainage and coalescence of drops in a viscous fluid. Macromol Mater Eng 296:238–248
36. Elmendorp JJ (1986) A study on polymer blending microrheology. PhD Thesis, Technical University of Delft
37. Janssen JMH (1993) Dynamics of liquid–liquid mixing. PhD Thesis, Eindhoven University of Technology
38. Fortelný I, Živný A (2003) Extensional flow induced coalescence in polymer blends. Rheol Acta 42:454–461
39. Fortelný I, Jůza J (2012) The effect of matrix elasticity on the shear flow induced coalescence of dispersed droplets. J Rheol 56:1393–1411
40. Jůza J, Fortelný I (2013) Flow induced coalescence in polymer blends. Chem Chem Technol 7:53–60